Ocean Modelling 27 (2009) 130–142

Contents lists available at ScienceDirect

Ocean Modelling

journal homepage: www.elsevier.com/locate/ocemod

Sensitivity of the Atlantic Ocean circulation to a hydraulic overflow parameterisation in a coarse resolution model: Response of the subpolar gyre

Andreas Born [a,*], Anders Levermann [a,b], Juliette Mignot [c]

[a] Potsdam Institute for Climate Impact Research, Potsdam, Germany
[b] Physics Institute, Potsdam University, Potsdam, Germany
[c] LOCEAN, Universite Pierre et Marie Curie, Paris, France

ARTICLE INFO

Article history:
Received 1 February 2008
Received in revised form 26 November 2008
Accepted 27 November 2008
Available online 13 December 2008

ABSTRACT

We investigate the sensitivity of a coarse resolution coupled climate model to the representation of the overflows over the Greenland–Scotland ridge. This class of models suffers from a poor representation of the water mass exchange between the Nordic Seas and the North Atlantic, a crucial part of the large-scale oceanic circulation. We revisit the explicit representation of the overflows using a parameterisation by hydraulic constraints and compare it with the enhancement of the overflow transport by artificially deepened passages over the Greenland–Scotland ridge, a common practice in coarse resolution models. Both configurations increase deep water formation in the Nordic Seas and represent the large-scale dynamics of the Atlantic realistically in contrast to a third model version with realistic sill depths but without the explicit overflow transport. The comparison of the hydrography suggests that for the unperturbed equilibrium the Nordic Seas are better represented with the parameterised overflows. As in previous studies, we do not find a stabilising effect of the overflow parameterisation on the Atlantic meridional overturning circulation but merely on the overflow transport. As a consequence the surface air temperature in the Nordic Seas is less sensitive to anomalous surface fresh water forcing.

Special attention is paid to changes in the subpolar gyre circulation. We find it sensitive to the overflow transport and the density of these water masses through baroclinic adjustments. The analysis of the governing equations confirms the presence of positive feedbacks inherent to the subpolar gyre and allows us to isolate the influence of the overflows on its dynamics.

1. Introduction

The submarine ridges between Greenland and Scotland (GSR) play a key role in the formation of North Atlantic Deep Water (NADW) (Gerdes and Köberle, 1995; Redler and Böning, 1997). Exchange between the Atlantic and the deep water formation sites in the Nordic Seas is limited and controlled by this barrier (Käse and Oschlies, 2000; Girton et al., 2006). The overflow over the ridge forms fast, buoyancy driven bottom currents. As it descends the southern slope of the GSR, the overflow mixes with the surrounding warmer North Atlantic waters to become NADW (Dickson and Brown, 1994; Hansen and Østerhus, 2000). Thus overflowing dense water plays an important role in the Atlantic meridional overturning circulation (AMOC) (Redler and Böning, 1997; Kuhlbrodt et al., 2007). The potential energy stored in the dense water reservoir in the Nordic Seas may have a stabilising effect on the AMOC (Lohmann, 1998) which is of great interest in the framework of climate change. A shutdown of the overflow transport and the successive reorganisation of the AMOC would weaken the heat transport to the high northern latitudes with strong implications for global climate (Vellinga and Wood, 2002). Sea level would rise by several decimetres in the North Atlantic (Levermann et al., 2005). Riemenschneider and Legg (2007) found oscillations in the overflow transport on a time scale of 4–5 days in a high resolution regional modelling study. On seasonal to interannual time scales the overflows are observed to be stable although the process of deep water formation in the Nordic Seas is highly seasonal because it depends on the strong winter cooling on the surface. Available direct observations of Nordic Seas overflows vary little on seasonal up to decadal time scales (Hansen and Østerhus, 2000). On the other hand, the Faeroe Bank Channel transport has been reported to show a decreasing trend for the second half of the 20th century (Hansen et al., 2001).

One characteristic of the overflows is the narrow passages by which they are formed. This causes their problematic representation particularly in coarse resolution models. In order to simulate the overflow transport these models typically use unrealistically deepened and broadened passages (Roberts and Wood, 1997; Thorpe et al., 2004). Here, we reassess this approach and compare it to a parameterisation by hydraulic constraints that follows

* Corresponding author. Present address: Bjerknes Centre for Climate Research, University of Bergen, Bergen, Norway. Tel.: +47 55 58 24 61.
E-mail address: andreas.born@bjerknes.uib.no (A. Born).

1463-5003/$ - see front matter © 2008 Elsevier Ltd. All rights reserved.
doi:10.1016/j.ocemod.2008.11.006

Kösters (2004), which was first implemented into a coarse resolution ocean model by Kösters et al. (2005). In their model, the parameterisation improves the representation of the overflows with realistic sill depths. Their parameterised model version compares well to the version with artificially deepened passages in equilibrium and under the influence of anomalous freshwater forcing in the North Atlantic.

In general, our experiments confirm the results of Kösters et al. (2005) regarding the effect on the meridional overturning. They give a first overview of the performance of the overflow parameterisation in comparison to a model version with realistic topography but no exchange across the GSR. We will focus on the difference between the two experiments where overflows are represented: the one including the parameterisation and the one with unrealistic topography. In particular, we observe a more intense subpolar gyre (SPG) with the explicitly represented overflows of the parameterisation. The analysis of the underlying mechanisms reveals that this is the consequence of baroclinic adjustments in the subpolar region due to different volume transport and density of the overflows. Surface wind stress has a strong influence on the SPG strength and variability (Curry et al., 1998; Böning et al., 2006). However, a number of studies emphasise the importance of the density structure on the gyre transport (Greatbatch et al., 1991; Myers et al., 1996; Penduff et al., 2000; Eden and Willebrand, 2001). Treguier et al. (2005) report large variations between different ocean models even though they are forced by the same wind stress. They find that SPG strength generally increases with model resolution. Our results suggest that this is partly due to the representation of the overflows, since it depends critically on the resolution in the GSR region.

We give a description of the model and the presented experiments in Section 2 and evaluate these experiments in Section 3. The differences in the SPG circulation are discussed in Section 4. In Section 5 we discuss our results.

2. Model description and experimental set-up

2.1. Model description

The parameterisation was implemented into the coarse resolution coupled climate model CLIM*BER*-3α (Montoya et al., 2005). CLIM*BER*-3α consists of the statistical–dynamical atmospheric model POTSDAM-2 (Petoukhov et al., 2000) coupled to a global, 24-layer ocean general circulation model based on the Geophysical Fluid Dynamics Laboratory (GFDL) Modular Ocean Model (MOM-3) code and to the dynamic and thermodynamic sea ice module of Fichefet and Maqueda (1997). The oceanic horizontal resolution is 3.75° × 3.75°. We apply a weak background vertical diffusivity of $0.2 \times 10^{-4}\,m^2/s$. For a discussion on the model's sensitivity to this parameter refer to Mignot et al. (2006). The implemented second-order moment tracer advection scheme (Prather, 1986) minimises numerical diffusivity (Hofmann and Maqueda, 2006). The model makes use of a parameterisation of boundary enhanced mixing depending both on near-bottom stratification and roughness of topography (Ledwell et al., 2000), following Hasumi and Suginohara (1999). This leads locally to vertical diffusion coefficients of up to $10^{-4}\,m^2/s$ for example over rough topography.

The atmospheric model has a coarse spatial resolution (7.5° in latitude and 22.5° in longitude) and is based on the assumption of a universal vertical structure of temperature and humidity, which allows reducing the three-dimensional description to a set of two-dimensional prognostic equations. Description of atmospheric dynamics is based on a quasi-geostrophic approach and a parameterisation of the zonally averaged meridional atmospheric circulation. The synoptic processes are parameterised as diffusion terms with a turbulent diffusivity computed from atmospheric stability and horizontal temperature gradients. Heat and freshwater fluxes between the ocean and the atmosphere are computed on the oceanic grid and applied without any flux adjustments. The wind stress is computed as the sum of the NCEP–NCAR reanalysis wind stress climatology (Kalnay et al., 1996) and the wind stress anomaly calculated by the atmospheric model relative to the control run.

2.2. Experimental set-up

The core of the present work is based on three different experiments. The first one models the overflows with an artificially deepened topography along the GSR and Iceland shifted eastward (DEEP). This unrealistic topography is the standard set-up of the model as described in Montoya et al. (2005) with a background vertical diffusivity of $0.2 \times 10^{-4}\,m^2/s$. The purpose of this set up was to artificially represent the overflow transport. The second experiment differs from DEEP in that the sills of the GSR region have their realistic depth (CTRL) and the third combines the same realistic topography with the hydraulic overflow parameterisation (HYDR) (Fig. 1). With this set-up we follow Kösters et al. (2005) but here we will focus on how the explicit representation of the overflows affects the large scale circulation compared to the enhancement of the across GSR flow achieved by deepening the sills.

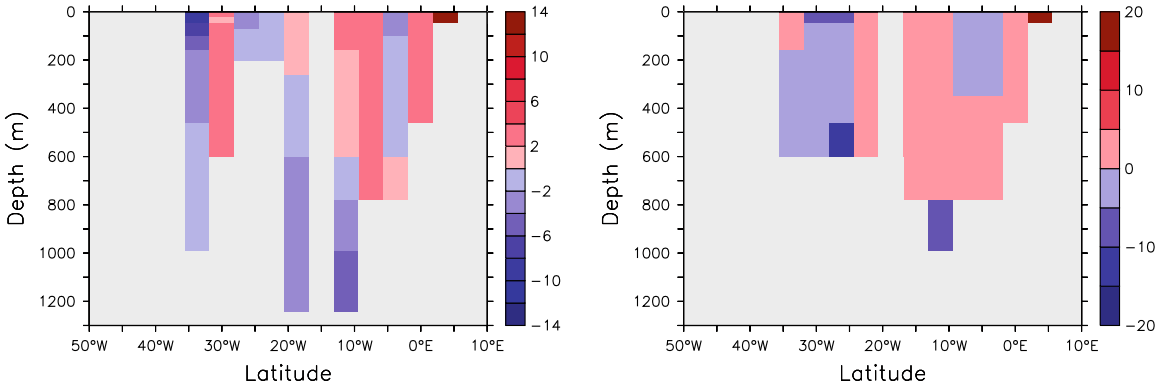

Fig. 1. Section along the Greenland–Scotland Ridge through Iceland (64° N). Colours: Meridional velocity component, negative means southward (cm/s). Left: topography and velocity of experiment DEEP with artificially deepened passages. The deep overflow transport occurs mainly through the deep passages between 20° W and 10° W. Right: topography of the experiments HYDR and CTRL with more realistic sill depths for the Denmark Strait and the Faeroe-Shetland Channel. The velocity shown is taken from experiment HYDR. The parameterised overflows are identified by the two grid cells with strong southward velocities. (For interpretation of the references to colour in this figure legend, the reader is referred to the web version of this paper.)

The theoretical basis of the parameterisation originates from the hydraulic theory of Whitehead et al. (1974). The overflow transport is computed from the large scale tracer distribution as proposed by Kösters et al. (2005):

$$Q_{\max} = \frac{g}{f\rho_0}\int_h^\eta (\rho_N(z) - \rho_S(z))z\,dz, \quad (1)$$

where $Q_{\max}$ is the maximum hydraulic overflow transport, defined as the integral from sill level depth h to the sea surface level η. ρ_N and ρ_S are the horizontally averaged but depth dependent densities north and south of the GSR. ρ_0, g and f are reference density, the gravitational constant and the Coriolis parameter. The integral represents the difference in average potential energy above sill level in two regions, north and south of the GSR. These regions were chosen to cover the whole Nordic Seas from the Greenland coast to 20° E and the entire North Atlantic in the latitude band between 45° N and the GSR at 64° N (Fig. 3, middle). As proposed by Kösters et al. (2005), we neglect contributions from the free surface layer and integrate the density differences from sill level to $z = 0$. The theoretically computed transport is added as an extra source in the momentum equation of the model grid cell of the sill (Fig. 1).

Kösters et al. (2005) report for their model that the parameterisation overestimates the overflows by about a factor of two (~6 Sv). They accept this discrepancy because a part of the overflow recirculates locally. Recirculation is weak in our model (Fig. 2), which might be due to the explicit free surface representation. However, in order to achieve a realistic representation of the North Atlantic hydrography and circulation the overflow transport has to exceed the observed values by a factor of two in our model as well. Note that the parameterisation ignores secondary effects like entrainment on sub-grid scale. Entrainment is believed to double the transport measured at the sills a few hundred kilometers downstream (Dickson and Brown, 1994). This length scale is comparable to the grid box size in our model and entrainment must thus be included in the parameterised volume transport. Indeed, the parameterised transport runs through a series of horizontal advection and vertical convection due to the stair-like representation of bottom slopes in our z-coordinate model. This further entrains surrounding water as it descends the GSR. We did not employ a bottom boundary layer advection scheme. The results presented here are multidecadal averages of experiments run into equilibrium for at least 2000 years.

3. Performance of the hydraulic overflow parameterisation

3.1. Effect of topography

The comparison of the two unparameterised model version, DEEP and CTRL, reveals major differences in the AMOC (Fig. 2). Over the artificially deepened passages in DEEP, overflows can pass the ridge in the southward direction and surface currents flow northward in order to compensate the outflow (Fig. 1). The East Greenland Current is represented by the southward surface flow along the coast of Greenland in our model. The inflow of saline water of tropical origin favours deep convection and an overturning circulation in the Nordic Seas (Figs. 2 and 3, see also Montoya et al. (2005)). With realistic topography the overturning circulation in the Nordic Seas stops and the AMOC is generally weaker (Fig. 2). Apart from a weak exchange by surface currents (not shown), the Nordic Seas are virtually disconnected from the North Atlantic. Because of the dense overflow water, NADW extends down to over 2700 m in DEEP with the deepest part on the southern slope of the GSR. The NADW overturning cell is shallower in CTRL, the GSR overflows do not exist here (Fig. 2). The most important difference in the horizontal circulation is a weaker SPG (Table 1).

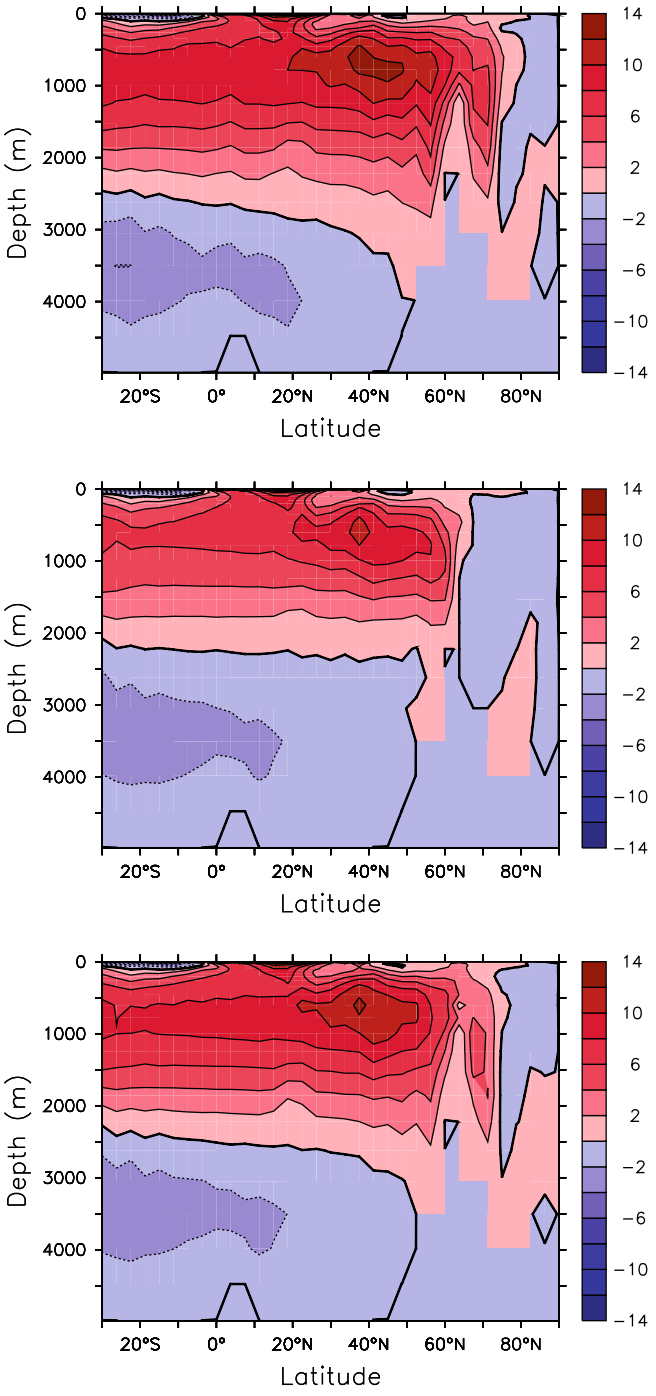

Fig. 2. Atlantic streamfunction for DEEP (upper), CTRL (middle) and HYDR (lower). Due to the GSR barrier (64° N), no exchange occurs between the North Atlantic and the Nordic Seas in CTRL. No meridional circulation is observed inside the Nordic Seas and it is weaker than in the other two experiments in the entire Atlantic. In HYDR, circulation in the Nordic Seas is weaker than in DEEP as well as the exchange over the GSR.

Ventilation is shallower, covers a smaller area and is located further south in the Nordic Seas in CTRL as compared to DEEP, as can be inferred from the shallower mixed layer depth (Fig. 3). South of the GSR, deep convection takes place further east than in DEEP. Due to the coarse resolution of our model deep convection in the Labrador Sea is shifted to Irminger Sea. However, the model does represent deep convection on both sides of the GSR and thus permits to study the effect of the overflow parameterisation on the large scale circulation.

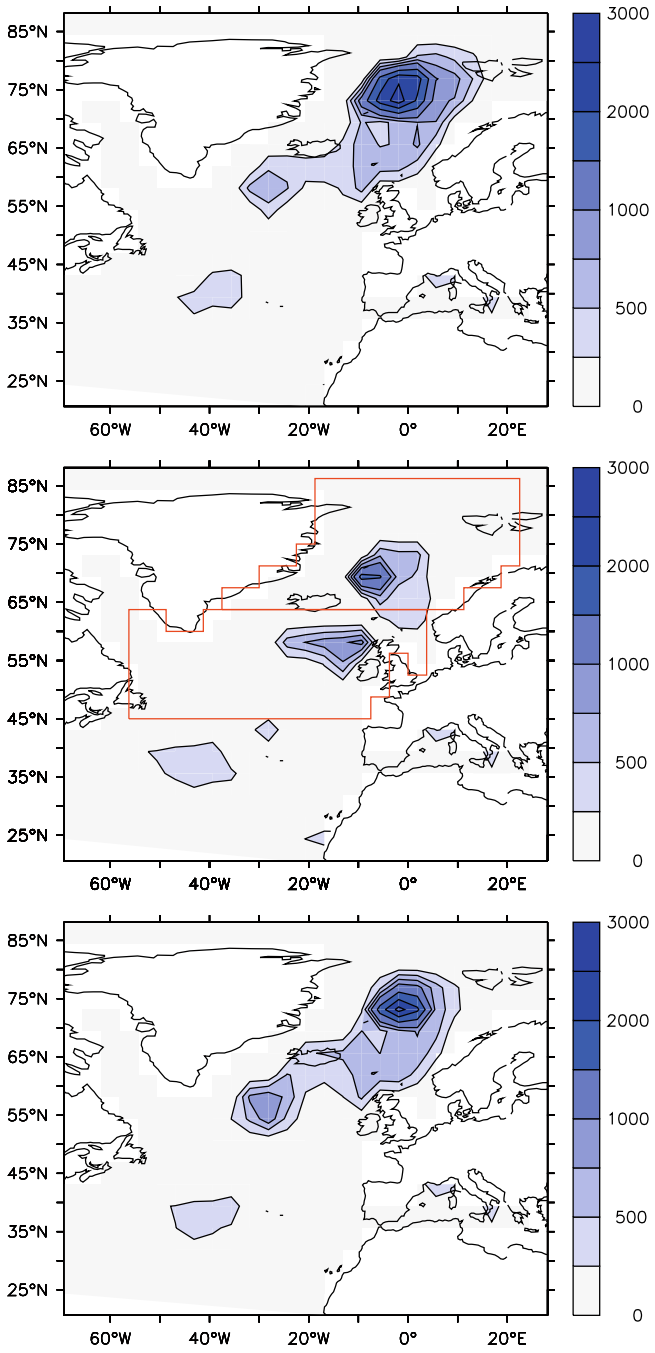

Fig. 3. Maximum winter mixed layer depth for DEEP (upper), CTRL (middle) and HYDR (lower). While in CTRL convection is weaker, DEEP and HYDR give similar results. In these two model versions convection takes place north of the GSR (64° N) and in the Irminger Basin southwest of Iceland. Note that our model does not show Labrador Sea deep convection due to the coarse resolution (Montoya et al., 2005). The red boxes show the regions where densities are averaged for Eq. (1). (For interpretation of the references to colour in this figure legend, the reader is referred to the web version of this paper.)

In CTRL the Atlantic Ocean is lighter at depth compared to DEEP and denser in shallower layers (Fig. 4, upper left). That is because deep waters are formed further south (south of Iceland). Furthermore, less warm and saline North Atlantic water reaches high latitudes in CTRL, where the overflows are much weaker. This agrees with observations that a large portion of the Atlantic inflow is due to a compensation of the overflow transport (Hansen and Østerhus, 2000). As a result, the relative impact of freshening by precipitation and run-off is more important and the Nordic Seas appear fresher (Fig. 4, lower left). South of the GSR, around 55° N, water is also lighter in CTRL. Denser waters above the GSR are associated with colder waters (Fig. 4 upper and middle left). This anomaly is due to intense atmospheric cooling while the weak advection in CTRL prevents the export of this water out of the region. In general, the patterns of differences in potential temperature and salinity, CTRL – DEEP (Fig. 4, middle and lower left) are similar because they are both affected similarly by the weaker deep water formation.

3.2. Effect of the overflow parameterisation

In HYDR deep convection occurs in roughly the same areas as in DEEP, mainly north of the GSR and partly in the Irminger Sea (Fig. 3). The Atlantic meridional overturning streamfunction is ~1 Sv weaker in the GSR region and in the Nordic Seas north of 64° N (Fig. 2). The overflow parameterisation restores the connection between the Nordic Seas and the North Atlantic compared to CTRL. The NADW overturning cell is deeper and stronger than in CTRL but still slightly shallower than in DEEP. The stronger overflows in DEEP as compared to HYDR are associated with a weaker downwelling south of the GSR (between 40° N and 64° N), which results in a comparable maximum of the AMOC (Fig. 2 and Table 1).

In HYDR, water masses below the maximum level of the zonally integrated streamfunction (compare Fig. 2, ~800 m) are denser than in DEEP throughout the Atlantic Ocean while in shallower layers lighter water is found (Fig. 4, upper right). The Nordic Seas between 64° N and 80° N are more stratified in HYDR than in DEEP (Fig. 4, upper right), surface waters are colder and fresher. As in CTRL, the relative contribution of river run-off and precipitation to the fresh water budget in the Nordic Seas becomes more important as a result of the weaker Atlantic inflow (Fig. 4, lower right). Because of the fresher surface waters, deep water formation requires stronger cooling in HYDR (see Fig. 4, right). Consequently, the potential temperature at depth is lower. However, the temperature below 500 m in the Nordic Seas is still higher than in the climatology (Fig. 5, middle right), which results in a lower density (Fig. 5, upper right). The salinity in the Nordic Seas is less than 0.1 psu higher in HYDR as compared to the Levitus (1982) climatology (Fig. 5, lower right), whereas in DEEP salinity is 0.1–0.2 psu higher (Fig. 5, lower left). This indicates that the strong exchange over the GSR as observed in DEEP (Fig. 2, upper) is not very realistic. It entails a strong ventilation of the Nordic Seas and hence too warm and saline water masses in this region especially at depth.

The most prominent difference between HYDR and DEEP is the dense water column around 55° N (Fig. 4, upper right). It reaches from the surface to 2500 m, the maximum depth reached by NADW in our model. It is related to the deeper mixed layer south of the GSR (Fig. 3) and a stronger subpolar gyre (Fig. 6) with about 10 Sv more volume transport in HYDR compared to DEEP (Table 1). In the meridional section, we observe a dipole in the temperature difference from the surface down to 1000 m (Fig. 4, middle right), centered at 55° N, which is also the centre of the SPG (Fig. 6). The dipole pattern is consistent with a stronger SPG as here warm and saline North Atlantic water reaches the northern side of the gyre and colder, fresher water of Arctic origin is advected to the South. The same pattern can also be found in the salinity section but here it is disrupted by a tongue of less saline water at ~300 m in HYDR that overlays the effect of the gyre (Fig. 4, lower right). The fresh water tongue results from a freshening of the Denmark Strait region (not shown). The sea surface elevation drops by more than 0.5 m in the centre of the SPG. However, this significant difference in the SPG circulation does not involve changes in the AMOC (Table 1 and Fig. 2), in contrast to previous work (Häkkinen, 2001).

Table 1
Properties of the Atlantic overturning circulation and the subpolar gyre for the three model versions. The depth of the NADW overturning cell is taken at the equator. Units are Sv ($=10^6$ m^3/s) and are taken from the zonally integrated streamfunction (Fig. 2) except for the subpolar gyre (SPG) strength which was calculated as the maximum zonal transport[a].

	AMOC maximum	Overflow	NA downwelling	SOO	NADW depth (m)	SPG
DEEP	13.16	7.29	5.87	10.34	2700	18.4
HYDR	12.55	3.92	8.63	9.65	2500	28.3
CTRL	10.92	2.48	8.44	6.94	2200	10.1

[a] Due to the explicit free surface, our model does not have a well defined vertically integrated (barotropic) streamfunction. Streamlines in following figures are for illustration purposes only.

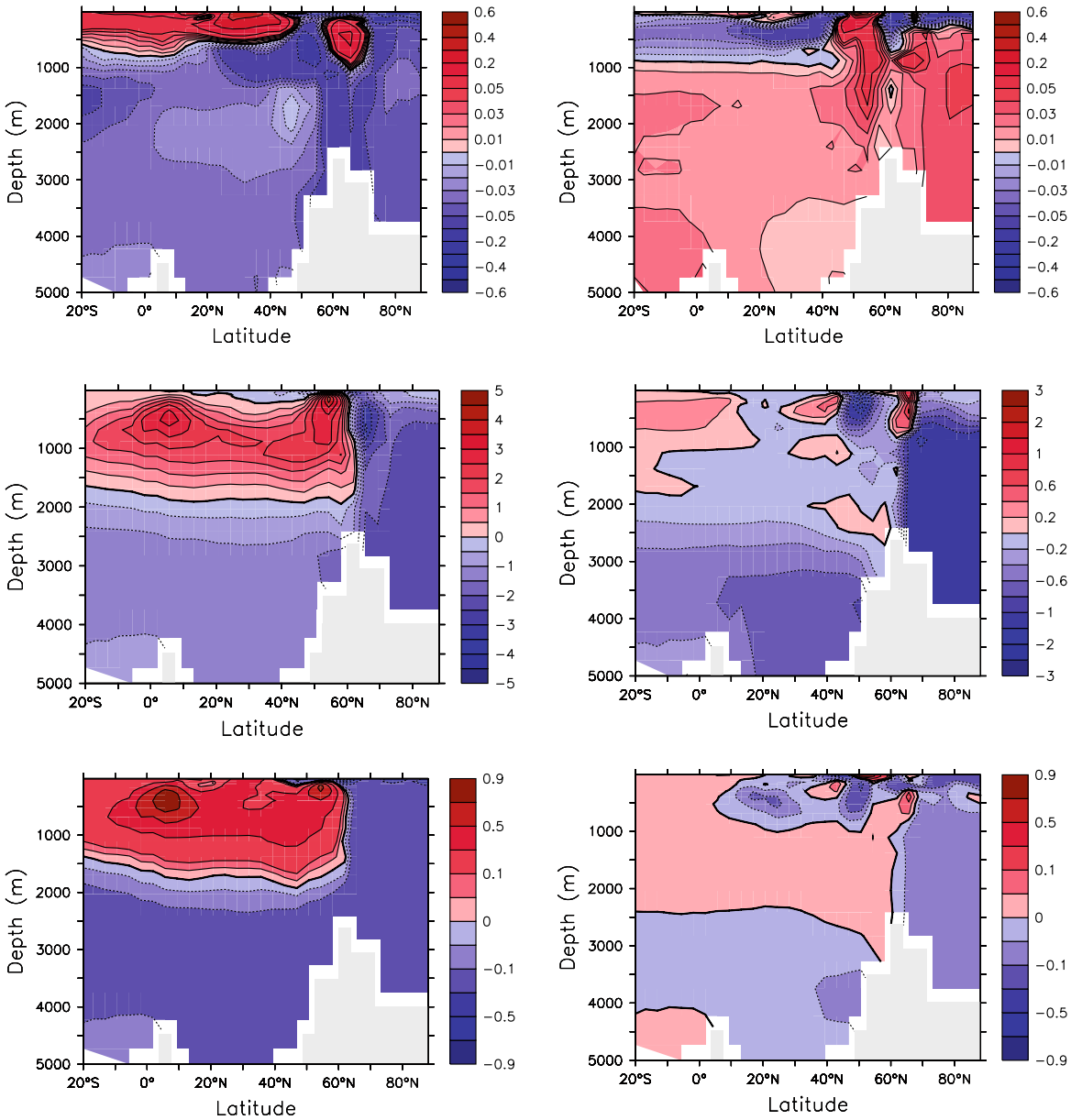

Fig. 4. Differences in the tracer distribution: left: CTRL − DEEP, right: HYDR − DEEP. The upper panels show the potential density (kg/m^3), the centered temperature (K) and the lower panels salinity (psu). The sections have been averaged zonally from 50° W to 30° E excluding the Mediterranean. Below 500 m, the Nordic Seas are warmer and fresher in HYDR than in the climatology.

The comparison of the two model configurations with the observational data reveals similar differences throughout the entire Atlantic (Fig. 5). Besides the density differences between deeper (below ~500 m) and upper water masses common in both experiments and the improvements in the Nordic Seas mentioned before, we observe a column of less dense water in the subpolar region in DEEP (Fig. 5, upper left, ~55° N). This anomaly on top of the general difference between upper and lower water masses is less pronounced in HYDR (Fig. 5, upper right). Temperature and salinity above 1000 m are closer to observations around 55° N in HYDR than in DEEP (Fig. 5, middle and lower).

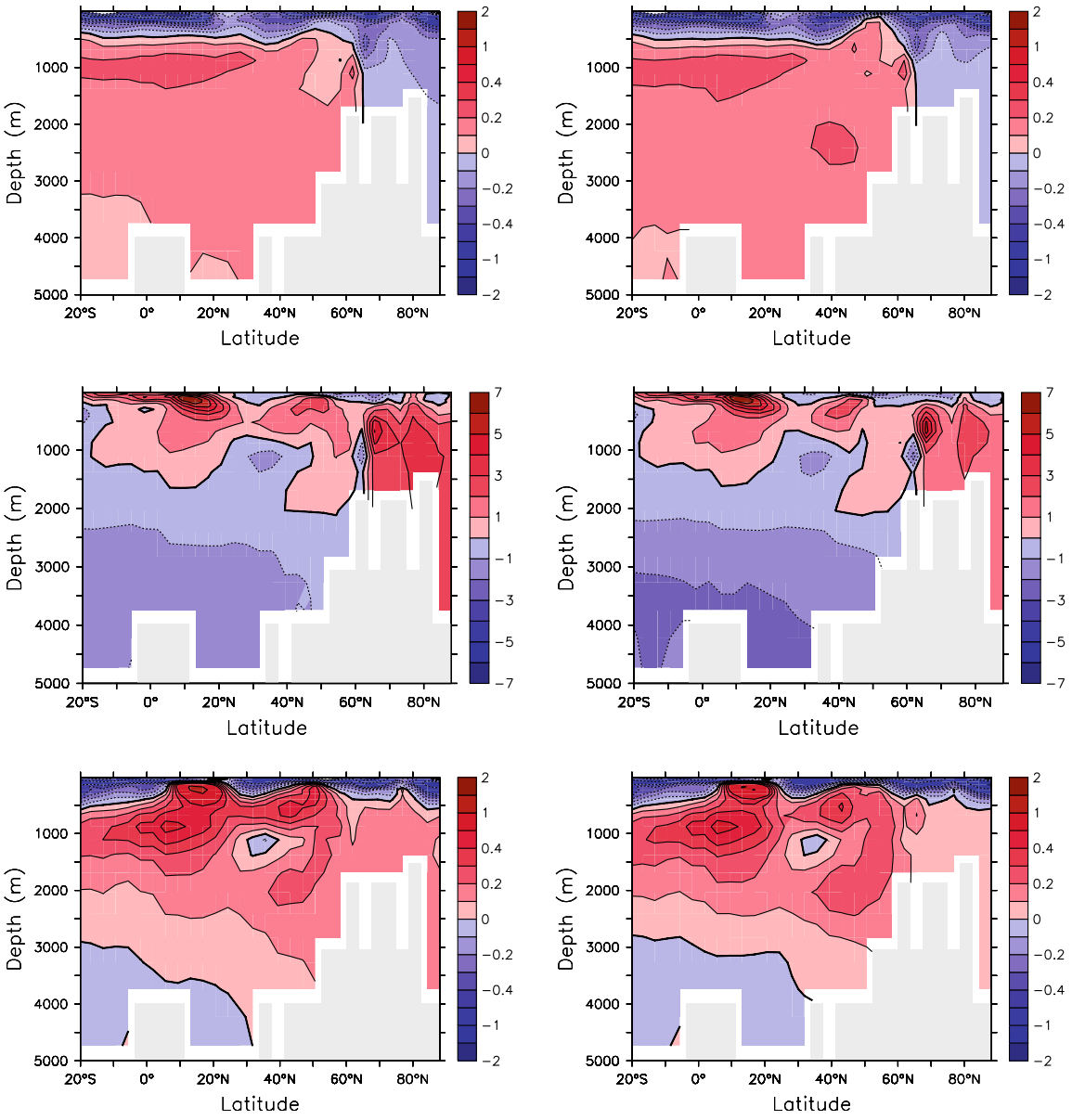

Fig. 5. Differences in the tracer distribution as compared to the Levitus (1982) climatology left: DEEP – LEVITUS, right: HYDR – LEVITUS. Upper: potential density (kg/m^3), middle: temperature (K), lower: salinity (psu). The sections have been averaged zonally from 50° W to 30° E excluding the Mediterranean.

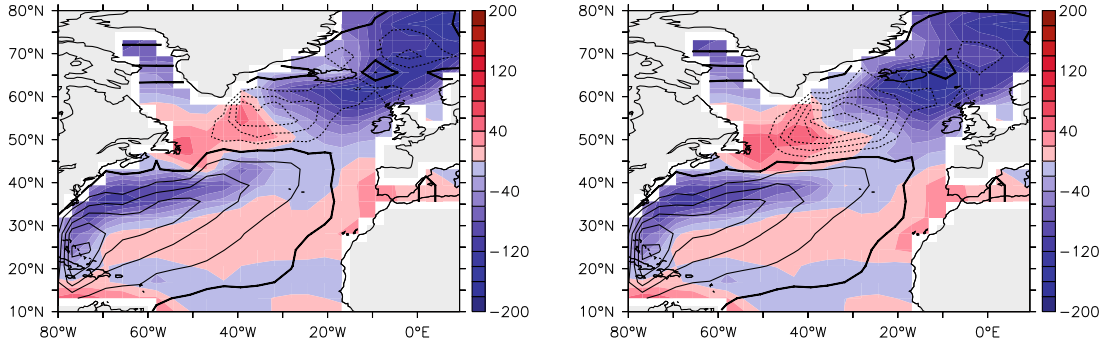

Fig. 6. Contours: streamlines of the vertically integrated circulation, barotropic streamfunction, contour levels spaced 5Sv. Colours: Heat flux into the ocean, negative values correspond to an oceanic heat loss. With the enhanced SPG in HYDR more heat is transported from the south-west end of the gyre to the north-east (compare with Fig. 7). Left for DEEP, right for HYDR, units are W/m^2. (For interpretation of the references to colour in this figure legend, the reader is referred to the web version of this paper.)

The different dynamics in the North Atlantic are reflected by the meridional heat transport. Due to the stronger SPG, more heat is transported by the horizontal circulation south of the GSR in HYDR (Fig. 7, green curve). The weaker meridional overtuning in this region (Fig. 2) also transports less heat (Fig. 7, red curve). However, this effect is overcompensated by the stronger SPG so that the meridional oceanic heat transport increases overall (Fig. 7, black curve). This can also be seen in the heat flux into the ocean (Fig. 6). In HYDR the ocean takes up more heat in the south-west of the SPG and looses more at its north-eastern side. At the latitude of the GSR (64° N) we observe a stronger heat transport (Fig. 7) by the overturning component in HYDR. We saw earlier that the meridional volume transport in this region is reduced (Table 1, overflow). However, the cooling is stronger in the Nordic Seas and hence the overflow water is colder in HYDR than in DEEP (Fig. 4, middle right). At the same time the stronger SPG provides warmer water at the surface and the overflow parametrisation forces the Atlantic inflow to a shallower path, so that it carries warmer surface water (Fig. 2). The more efficient heat transport is the result of this bigger temperature contrast between surface inflow over the GSR and deep outflow.

We conclude that the overflow parametrisation in HYDR restores deep convection in the Nordic Seas and exchange with the North Atlantic as has previously been reported for another global coupled model by Kösters et al. (2005). We can also confirm their finding that the explicit representation of the GSR overflows has only a small impact on the AMOC strength. They find an increase of the AMOC of ~1 Sv between the reference model version with realistic topography and the parameterised model. In our model, this corresponds to the difference of ~1.5 Sv between HYDR and CTRL. Apparently, this result is independent of the precise location of deep water formation, because we observe a strong increase in deep convection in the Nordic Seas and the centre of the SPG in HYDR while Kösters et al. (2005) report only a modest increase accompanied by a reduction south of the GSR.

Kösters et al. (2005) report an increase of 2 Sv in the SPG circulation from their unparameterised reference experiment to the parameterised version, which must be compared to the 18 Sv, or nearly threefold, increase we observe between CTRL and HYDR. They do not state a significant increase for the parameterised model. This influence of the GSR overflows on the SPG as opposed to the lack of their representation, is well known and has been reported repeatedly. Model studies by Roberts and Wood (1997), Redler and Böning (1997) and Penduff et al. (2000) indicate that the outflow of dense water from the Nordic Seas enhances the SPG circulation compared to model versions where this outflow is missing.

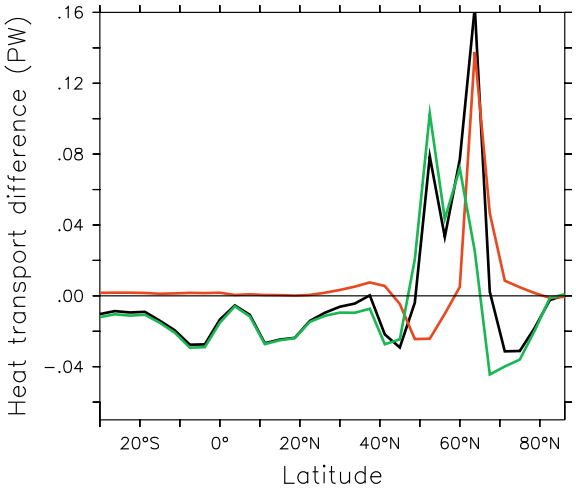

Fig. 7. Difference in the northward heat transport, HYDR – DEEP (black), decomposed into an overturning and a gyre transport (zonally averaged transport and its deviation, red and green curves, respectively). Units are PW (=10^{16} W). (For interpretation of the references to colour in this figure legend, the reader is referred to the web version of this paper.)

Among the two experiments with overturning circulation in the Nordic Seas, DEEP and HYDR, the latter shows an improved representation of water masses in the Nordic Seas and the subpolar Atlantic. While the representation of the meridional circulation is similar in these two model versions, HYDR shows a stronger SPG associated with hydrographic changes in the region. This difference of 10 Sv (Table 1) between two different but equivalent representations of the overflow transport has not been observed in previous model studies. We will address this subject more in detail in Section 4.

3.3. Response to anomalous freshwater flux

In order to understand how the hydraulic overflow parameterisation changes the stability of the oceanic circulation, we analyse a series of experiments with anomalous freshwater flux to the North Atlantic. The anomalous freshwater flux is applied continuously as a negative salt flux for 1000 years in the latitude band from 20° N to 50° N in the Atlantic Basin. Only the equilibrium response of the two model versions is considered. For a detailed stability analysis of the AMOC in DEEP including the response to different forcing regions see Gölzer et al. (2006).

The weakening of the maximum of the AMOC is similar for HYDR and DEEP for the same anomalous freshwater flux (Fig. 8). On the other hand, the overflow strength behaves differently. While in DEEP the overflows weaken about the same in absolute values as the AMOC, they are much more stable in HYDR. We see that for high anomalous freshwater fluxes (above 0.2 Sv) the overflows in DEEP stop (Fig. 8) and the entire deep water formation takes place south of the GSR. This does not happen in HYDR where the overflow transport is relatively stable over the presented interval of fluxes.

Since the AMOC reduction is similar in both DEEP and HYDR, this difference in overflows response has consequences for deep water formation south of the GSR: The maximum AMOC is related to a meridional density gradient in the Atlantic (Rahmstorf, 1996; Levermann and Griesel, 2004). An anomalous freshwater flux weakens this gradient and consequently the overturning circulation in HYDR and DEEP similarly. In this view, downwelling in the high northern latitudes has to adapt to the volume transported in the AMOC. Water masses advected northward in the surface limb of the AMOC that do not sink in the Nordic Seas must sink further south between 40° N and 64° N in the North Atlantic (see Fig. 2). Since most of the water entering the Nordic Seas with the Atlantic inflow sinks in this basin and returns to the North Atlantic in the overflows (Hansen and Østerhus, 2000), the overflow transport is a good estimate for the deep water formation in the Nordic Seas. Consequently, more stable overflows in HYDR yield the stabilisation of the Nordic Seas deep water formation and thus a greater weakening of deep water formation south of the GSR than in DEEP, where for freshwater fluxes above 0.3 Sv the entire deep water formation takes place south of the GSR. More stable overflows are thus finally linked to more vulnerable deep water formation south of the GSR.

In order to understand the greater stability of the overflows in HYDR, we consider the experiments with 0.2 Sv anomalous freshwater flux, in which the overflow strength is equal in DEEP and HYDR (Fig. 8). Salinity changes in the Nordic Seas as compared to the respective nonperturbed experiments are weaker in HYDR because of the Atlantic inflow: it enters the Nordic Seas as a surface current while in DEEP it flows at intermediate depths. This is seen

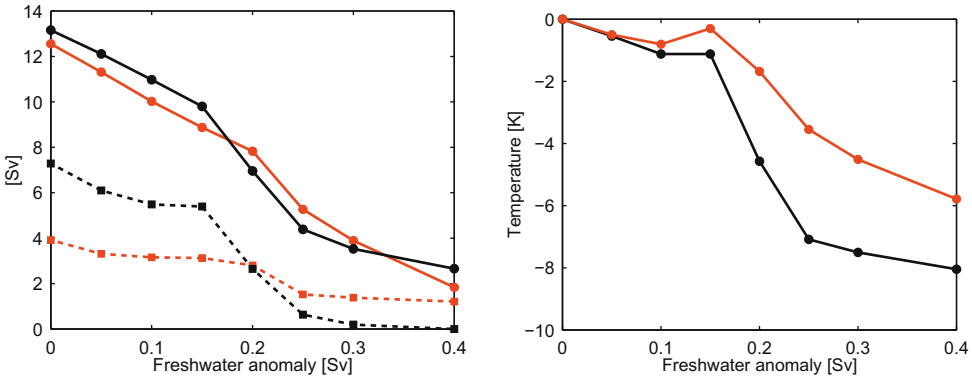

Fig. 8. A continuous negative salt flux was applied to the latitude band between 20° N and 50° N, black: DEEP, red: HYDR. Left: maximum overturning strength (solid) and overflow volume (dashed) as function of the freshwater anomaly. Right: surface air temperature anomaly in the Nordic Seas, the region is shown in Fig. 10. Because the overflow transport and hence the deep water formation in the Nordic Seas is more stable in HYDR, downwelling south of the GSR is more sensitive to the anomalous freshwater flux (not shown). Due to the stability of the overflows the temperature in the Nordic Seas changes less in HYDR. (For interpretation of the references to colour in this figure legend, the reader is referred to the web version of this paper.)

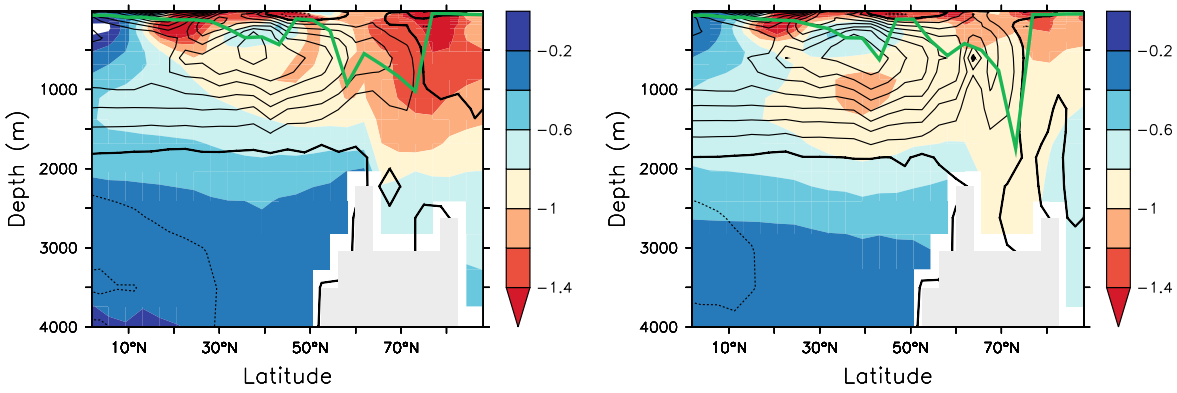

Fig. 9. Salinity changes in the experiments with 0.2 Sv anomalous freshwater flux into the North Atlantic compared to their respective equilibrium experiment, units are psu, DEEP left, HYDR right. In DEEP the Nordic Seas freshen more than in HYDR although the overflow transport is equal in both experiments (Fig. 8). This is due to the shallower Atlantic Inflow in HYDR seen in the contours for the perturbed experiments. Green curve shows the zonal maximum of the maximum winter mixed layer depth, which is deeper in HYDR in the Nordic Seas. (For interpretation of the references to colour in this figure legend, the reader is referred to the web version of this paper.)

in the contours of the streamfunction. In HYDR a flux of 2 Sv takes place in the upper 100 m while in DEEP it is spread over 400 m (Fig. 9). Thus it advects more saline water to the high latitudes and also more heat which is released to the cold atmosphere. The enhanced surface flow in HYDR compared to DEEP favours a destabilisation of the water column and therewith deep convection. Thus, deep convection in the Nordic Seas is stronger in HYDR for an anomalous freshwater flux of 0.2 Sv (Fig. 9). Sea ice reaches further south and tends to close the Nordic Seas along the GSR at 64° N in DEEP but not in HYDR (Fig. 10). This further weakens the strength of the atmosphere ocean interaction in DEEP and deep convection. Consequently, surface air temperature differs by ~2 K from the equilibrium in HYDR and more than 6 K in DEEP (Fig. 10, 4 K on regional average, Fig. 8) in the experiment with 0.2 Sv anomalous freshwater flux. The changes in subsurface temperatures implied by the shallower Atlantic inflow might play an important role in the rate of recovery after the anomalous freshwater forcing (Mignot et al., 2007).

4. Dynamics of the subpolar Atlantic Ocean

4.1. Vorticity balance in the subpolar gyre

The analysis of the properties of the subpolar Atlantic Ocean revealed major differences between the model versions that represent the overflow transport in two different ways, HYDR and DEEP. We found that the hydrographic changes in the North Atlantic region in HYDR are accompanied by a more intense SPG (Section 3.2). In order to understand how the overflow parameterisation affects the circulation pattern in this region, we have to revisit the dynamics of the SPG.

We define the gyre transport as the horizontal advection in the entire water column. Consider the depth integrated volume transport equation in zonal direction (derived in Appendix A),

$$fM_x = -H\partial_y P_b + \partial_y \Phi + \frac{\tau_{0y}}{\rho_0} \tag{2}$$

with

$$P_b \equiv g\eta - \int_{-H}^{0} dz'\, b',$$

$$\Phi \equiv \int_{-H}^{0} dz z \cdot b.$$

The term $\rho_0 P_b$ is the bottom pressure and $\rho_0 \Phi$ the potential energy at depth H. For the depth-integrated two-dimensional flow in (2), the left-hand side and the first term on the right-hand side represent a geostrophic balance. An amplification of the SPG flow can only be due to the ageostrophic contributions from the potential energy and the wind stress terms, as can also be seen in the

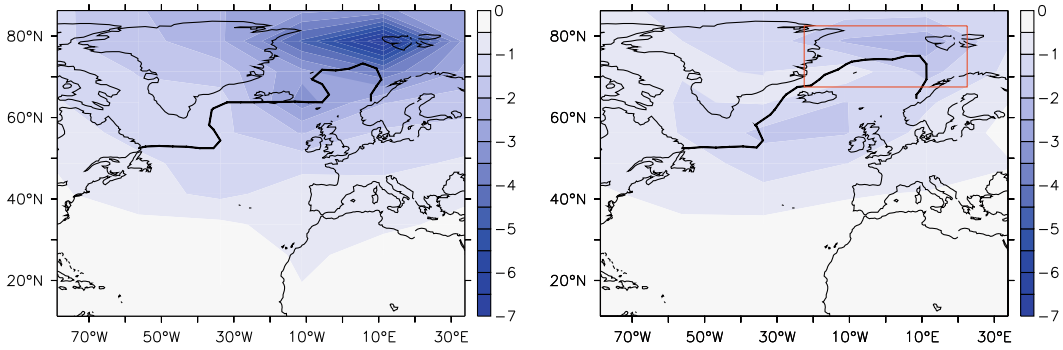

Fig. 10. Surface air temperature difference to the respective unperturbed experiment (in K) DEEP (left) and HYDR (right) with anomalous freshwater flux (0.2 Sv). The heavy contour line shows the maximum winter sea ice extent (>50% sea ice cover). Note that in DEEP sea ice tends to close the Nordic Seas even with an ongoing circulation below the surface (Fig. 9). In HYDR the overflow transport is equal in strength but due to the overflow parameterisation in shallower depths. The region used for the temperature average in Fig. 8 is marked red. (For interpretation of the references to colour in this figure legend, the reader is referred to the web version of this paper.)

barotropic vorticity equation. We cross differentiate Eq. (2) and its counterpart for the meridional transport and add them up to obtain

$$\mathbf{M}\cdot\nabla\left(\frac{f}{H}\right) = M_x\partial_x\left(\frac{f}{H}\right) + M_y\partial_y\left(\frac{f}{H}\right) = H^{-2}(\partial_y H\partial_x\Phi - \partial_x H\partial_y\Phi) + \partial_x\left(\frac{\tau_{oy}}{\rho_0 H}\right) - \partial_y\left(\frac{\tau_{ox}}{\rho_0 H}\right). \quad (3)$$

The left hand term is the vertically integrated mass transport across f/H contours. The bottom pressure term has been eliminated and the two remaining terms represent the joint effect of baroclinicity and relief (JEBAR; Sarkisyan and Ivanov, 1971; Mertz and Wright, 1992; Cane et al., 1998) and the surface wind stress curl. Eq. (3) can also be interpreted as a vorticity balance. The JEBAR describes a vorticity input to the ocean due to variations in the potential energy supported by a sloping topography. In a flat ocean the JEBAR vanishes. Since the bottom pressure term is not part of this vorticity balance, it cannot contribute to a more intense SPG circulation.

4.2. Dominance of the potential energy term

The bottom pressure term can be disregarded as the reason for the SPG spin-up because it does not create vorticity in the ocean. Now consider the contribution of each of the two remaining source terms on the right-hand side of Eq. (3). We observe a stronger vorticity input in HYDR than in DEEP due to the JEBAR (Fig. 11, left). It creates positive vorticity south of Denmark Strait (~25° W, ~60° N) which is consistent with a stronger cyclonic SPG circulation. On the other hand, the difference of the vorticity input from the wind stress curl is minor (Fig. 11, right). This already indicates the importance of the overflow transport on the SPG circulation in our model. It is important to note that this term depends on the vertical density distribution $z\cdot b$ and the local ocean depth H. Since the topography remained unchanged outside the sills of the GSR, the observed changes must be due to the changed density distribution alone. The dominance of the potential energy over the wind stress term can also be seen in the zonal transport (Eq. (2)), which we will use for the following qualitative analysis.

The zonal transport contribution due to the difference in potential energy ($f^{-1}\partial_y\Phi$, Eq. (2)) between HYDR and DEEP is shown in the upper left of Fig. 12. Positive values indicate a stronger eastward transport in HYDR as can be observed in the southern half of the SPG. In its northern limb, a stronger westward transport conveys more water in the opposite direction. The difference in the contribution of the wind stress is negligible (Fig. 12, upper right). The difference of the vertically integrated zonal transport derived from the model's simulated velocities is shown on the lower left of Fig. 12. Note that large changes in the potential energy and the observed model velocities are confined to the subpolar region. Their spatial pattern as well as the absolute values of the inferred transports are similar. Contours are for the barotropic streamfunction in HYDR and demonstrate the spatial collocation of the transport anomalies and the SPG.

Besides the spatial agreement, the difference in the potential energy term explains the strength of the circulation change also quantitatively. The meridionally integrated contribution of the potential energy to the zonal transport ($f^{-1}\partial_y\Phi$) gives a measure for the gyre transport due to the potential energy term. It explains a difference (HYDR – DEEP) of roughly 10 Sv (Fig. 12, lower right, black curve). This is close to the difference in the gyre strength inferred similarly from the vertically integrated zonal velocities (red

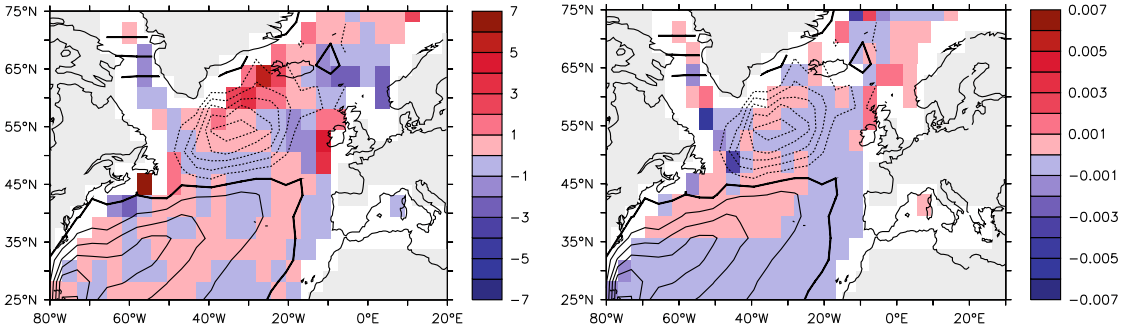

Fig. 11. Left: difference in the JEBAR between HYDR and DEEP. Please note the positive anomaly south of the Denmark Strait in HYDR compared to DEEP. Right: the difference in the wind stress curl is three orders of magnitude smaller and hence negligible. Units are 10^{-12} s^{-2}. Contour lines show the barotropic streamfunction in HYDR.

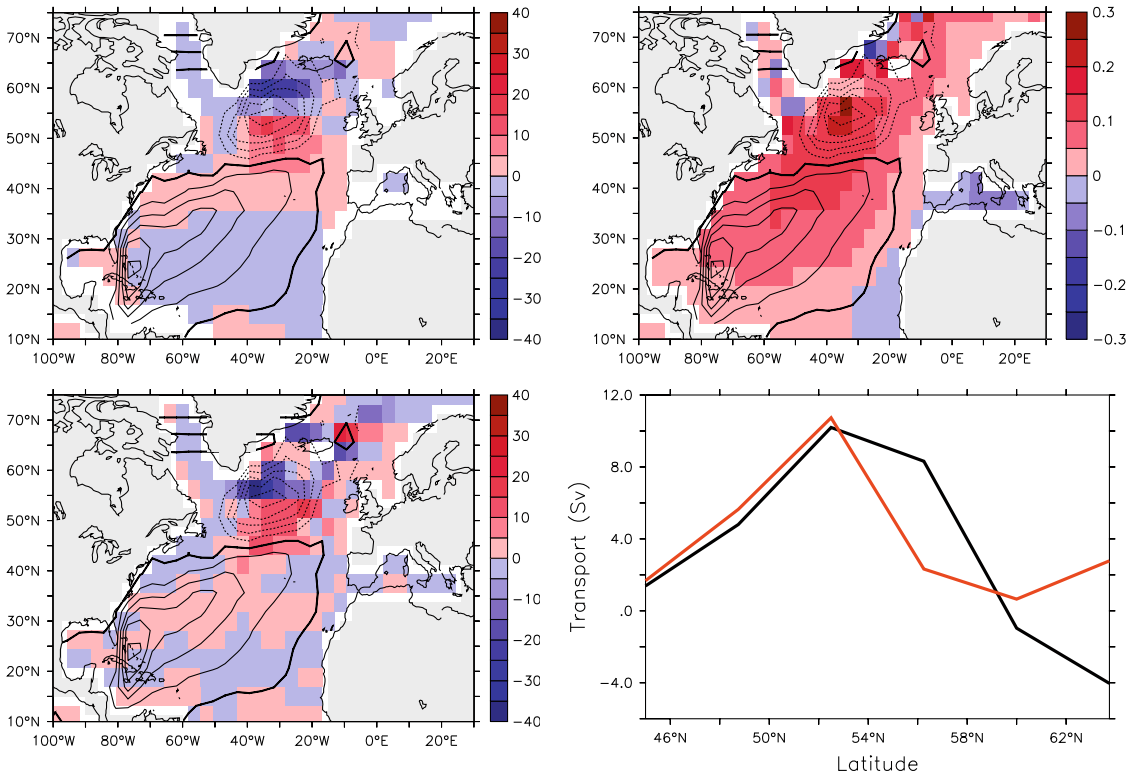

Fig. 12. Differences HYDR − DEEP in the vertically integrated, zonal transport. Positive values indicate eastward transport (m^2/s), contours are stream lines of the vertically integrated transport in HYDR and demonstrate the spatial agreement of the changes with the SPG. Upper left: vertically integrated zonal transport as computed from the potential energy term ($f^{-1}\partial_y \Phi$). Lower left: vertically integrated zonal transport as derived from the model's simulated velocities, upper right: Difference in the vertically integrated zonal transport due to changes in the wind stress. Differences in wind stress are small as compared to those shown on the left side and do not reproduce the gyre structure, in contrast to the differences due to baroclinicity. Lower right: vertically integrated transport as shown in left panels, zonally averaged over the gyre centre (40–20° W) and meridionally integrated in order to obtain a measure of the gyre strength difference. The black curve corresponds to the transport derived from the density field (upper left), the red one to the simulated velocities (lower left). The curves disagree near the Greenland coast due to the neglected friction terms in Eq. (2). The maximum value in the gyre centre is in good agreement (10 Sv). (For interpretation of the references to colour in this figure legend, the reader is referred to the web version of this paper.)

curve and Table 1). Both fields have been zonally averaged over the centre of the gyre (40–20° W) before the integration from south to north. The two curves show good agreement except near the Greenland coast where the neglected effect of friction becomes dominant. They begin to diverge at 56° N, the latitude of Cape Farewell in our model. The comparison confirms that the main difference of SPG strength between HYDR and DEEP is due to changes in the baroclinic potential energy term.

4.3. The role of the overflows

The interpretation of the second term in Eq. (2) as potential energy helps to understand the impact of the overflows on the subpolar gyre. The contour plot in Fig. 13 shows a range of density isolines zonally averaged over the SPG centre (40–20° W). Their slope can be used to evaluate qualitatively the derivative of the potential energy that enters equation (2) (second term) and drives the SPG. A stronger outcropping of the isopycnals is equivalent to a more intense gyre circulation. While the isopycnal maxima in HYDR are all at the same latitude, in DEEP they are displaced to the south with increasing depth. Above 800 m, the steeper rise of the isopycnals between 40° N and 55° N is the cause for the more intense eastward transport in HYDR in the southern half of the SPG. On the northern side of the gyre the isopycnal gradient is negative, resulting in an enhanced westward transport. In DEEP the isopycnals neither rise as much nor fall notably. Isopycnals below 800 m are smoother but the density derivative becomes more important with increasing depth due to the weight of the depth z in the potential energy term ($z \cdot \partial_y \rho$, colour[1] shading in Fig. 13). At these depths, the most significant difference between the two experiments is the positive isopycnal gradient in DEEP on the southern slope of the GSR around 60° N due to the more intense overflow transport over the ridge.

Thus, the overflow transport partly controls the SPG circulation because it changes the meridional density gradient south of the GSR, the rim of the SPG. However, the largest increase of the centre-to-rim density gradient below 800 m is due to a density increase in the centre of the gyre (0.06 kg/m^3), not the decrease on its rim (−0.01 kg/m^3). This is the result of two positive feedback mechanisms inherent to the SPG. First, the stronger outcropping of the isopycnals makes isopycnal mixing of heat to depth and out of the gyre's centre more efficient (Fig. 14, left). Secondly, a stronger gyre results in less salt transport into the Nordic Seas (Hátún et al., 2005) and hence accumulation of salt in the subpolar North Atlantic which again increases the density of the gyre centre (Figs. 4 and 14, right) (Levermann and Born, 2007). Thus, the overflow transport parameterisation does not increase the SPG strength directly but favours the development of positive feedbacks. It is, however, not possible to quantify a minimum necessary overflow change in this study because the overflows have been represented in two fundamentally different ways.

[1] For interpretation of the references to colour in Fig. 13, the reader is referred to the web version of this paper.

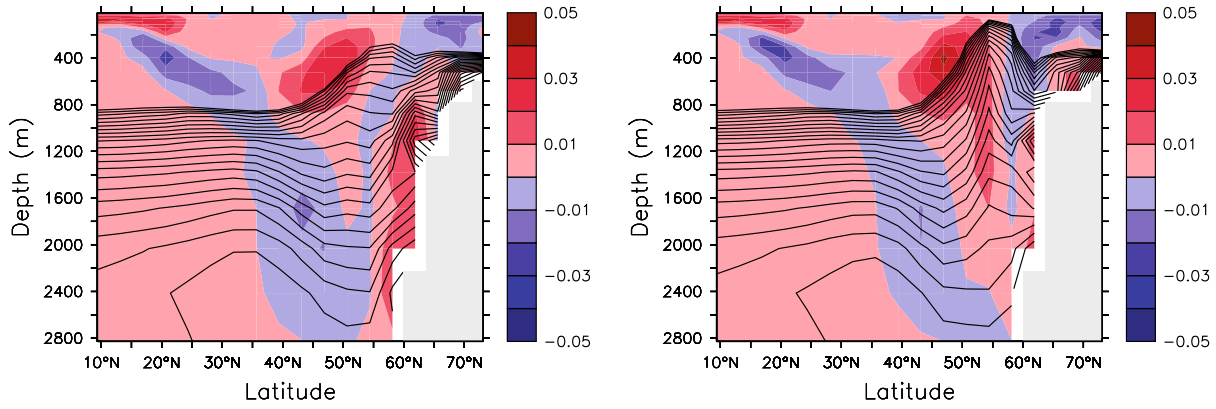

Fig. 13. Meridional density gradient weighted by depth, $z \cdot \partial_y \rho$, averaged over the SPG centre (40–20° W). It provides a measure of the zonal transport due to the JEBAR (see Eq. (2)). Left: DEEP, right: HYDR. The contours show a certain range of the corresponding isopycnals. With the stronger gyre in HYDR, more isopycnal outcropping is seen and the domed structure is maintained over the entire depth. The separation between the positive (eastward) around 55° N and negative (westward) forcing around 60° N is also more pronounced. Intense overflow transport in DEEP causes a eastward transport on the GSR slope between 800 and 2500 m. Units are arbitrary as we focus on the sign only.

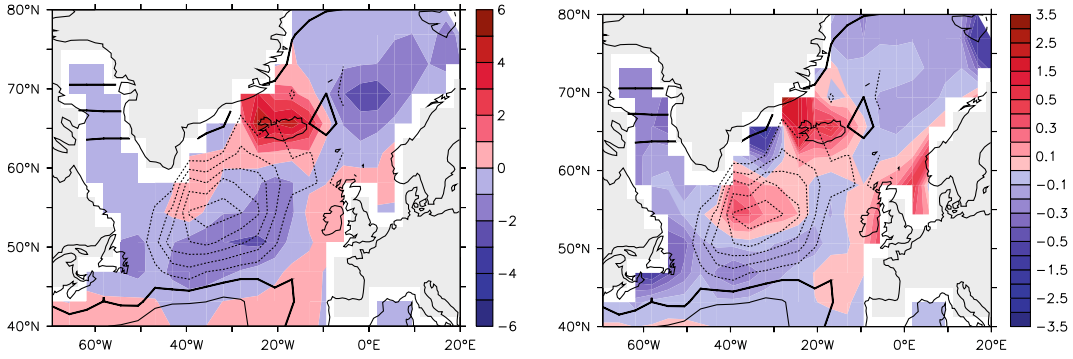

Fig. 14. Temperature (left) and salinity (right) differences HYDR – DEEP in the North Atlantic and Nordic Seas, averaged over the upper 1000 m, units are K and psu, respectively. Contours: stream lines of the SPG in HYDR. The centre of the gyre is colder and more saline in HYDR which results in a higher density (compare with Fig. 4). We also observe a stronger deep convection in this region in HYDR (Fig. 3).

5. Conclusion and discussion

A parameterisation for the Nordic Seas overflow by hydraulic constraints was implemented in a coarse resolution climate model. We can confirm the finding of Kösters et al. (2005) that this parameterisation overcomes the problem of a missing exchange over a realistically represented GSR. In contrast, simulations with realistic topography but unparameterised overflow (CTRL) yielded unsatisfactory results.

Between the model version with explicitly parameterised overflows (HYDR) and the version with deepened topography (DEEP) we see relatively small differences in density in the Atlantic basin because the parameterised overflows are not only denser but also weaker in HYDR. Since the weaker overflows are accompanied by a weaker Atlantic inflow into the Nordic Seas, the Nordic Seas ventilation is weaker in HYDR than in DEEP. This permits the formation of denser water masses. The stronger exchange across the GSR in DEEP results in warmer and more saline water in the deep Nordic Seas, at odds with observations. Temperatures and salinities in this basin are closer to observed values in HYDR and suggest that the dynamics of the GSR region for the present-day climate are better represented in HYDR.

The application of an anomalous freshwater flux to the North Atlantic revealed major differences in the stability of the overflow transport, but not in that of the AMOC in general. The parameterisation stabilises the overflows. In DEEP the overflow transport breaks down for an anomalous forcing above 0.2 Sv while in HYDR it remains even with stronger forcing. With the overflow parameterisation the Atlantic inflow is concentrated on the surface and thus warmer and more saline. Consequently, the Nordic Seas freshen less in HYDR, the sea ice edge is further north and deep convection in this region is more stable than in DEEP. The surface air temperature in the Nordic Seas decreases less with increasing anomalous freshwater flux. The shallower Atlantic inflow changes subsurface temperatures in the Nordic Seas. These were recently found to be important for the destabilisation of the water column and the rate of recovery of the overturning circulation after the anomalous freshwater forcing (Mignot et al., 2007). Therefore, and because of the enhanced stability of the overflows, the parameterisation might have consequences for the model-based understanding of climate dynamics and palaeoclimatic events.

A notable influence of the overflow parameterisation is found in the strength of the SPG, which is 28 Sv in HYDR, about 10 Sv stronger than in DEEP. This is a reasonable value according to measurements by Bacon (1997), who found a gyre transport of 25–27 Sv. Clarke (1984) derived a higher value of 33.5 Sv from a section across the western SPG where recirculation inside the Labrador Sea and the deep western boundary current, part of the AMOC's southward flowing branch, may explain the stronger transport. High resolution models tend to show an even more vigorous circulation of order 30–50 Sv (Treguier et al., 2005). Our experiments suggest that this is related to the more detailed representation of the GSR overflows in higher resolved models. The comparison of the hydrography of HYDR and DEEP with the climatology by

Levitus (1982) also implies that the deep water formation in HYDR associated with the stronger gyre is a better representation of the subpolar region.

In the analysis of the mechanisms underlying the stronger SPG circulation we found baroclinic adjustments through the JEBAR to be the dominant difference. This is in agreement with Greatbatch et al. (1991) and Myers et al. (1996) who found the SPG entirely controlled by JEBAR. Penduff et al. (2000) came to the same conclusion and state that in their model JEBAR clearly dominates over all contributions able to generate transport across f/H isolines. In a study of interannual to decadal variability of the North Atlantic circulation Eden and Willebrand (2001) found the enhancement of the SPG of about 2 Sv 2–3 years after seasons of strong convection in its centre, which they relate to the JEBAR.

We identified two mechanisms that control the SPG strength through baroclinicity. The first one is an auto-intensification that increases the density in its centre due to changes in heat and salt transports. The second mechanism is related to the GSR overflows and the formation of NADW on the GSR slope. Although its influence on baroclinicity in the North Atlantic is smaller than the one from the internal feedback mechanisms, it does not depend as strongly on the SPG circulation strength as the latter. Hence it provides an external control mechanism and triggers changes in the SPG transport. The experiments with explicitly represented overflow transport shown here support this view originally presented by Levermann and Born (2007) for the model version with artificially deepened passages (DEEP). We complement their qualitative discussion with the theoretical background presented in Section 4.

One limitation of our model is that due to its coarse resolution deep convection is shifted from the Labrador Sea to the Irminger Sea. As a consequence, the SPG does not enter Labrador Sea and neither does the deep western boundary current that is fed by the overflow waters turning westward after passing the GSR. However, our model consistently simulates the large scale circulation: convection occurs inside the SPG and a cyclonic boundary current embraces the deep convection area.

Wood et al. (1974) state that a lighter overflow water mass weakens the cyclonic circulation in the Labrador Sea, seemingly contradicting our findings. Note, however, that their statement concerns the Deep Western Boundary Current, while we describe the circulation in the upper 1000 m. Observations (Häkkinen and Rhines, 2004), high resolution model studies (Spall, 2004) as well as theoretical considerations (Straneo, 2006) strongly suggest that a stronger SPG is associated with doming isopycnals in its centre and that an enhanced density gradient between centre and exterior strengthens the SPG circulation. This is indeed consistent with Wood et al. (1974) in which an existing gyre circulation is associated with a denser gyre centre compared to the exterior and the cyclonic SPG circulation collapses when this density differences are eroded. We are thus confident that we capture the basic characteristics of the dynamics of the North Atlantic subpolar basin correctly despite the shortcomings in resolution.

Another limitation is the relatively simplified atmospheric model, which does not allow for variability. The overflow parameterisation proved to be robust in the experiments with anomalous freshwater flux. The mechanisms related to heat and salt transport inside the SPG depend on large scale properties of the circulation only. Therefore, decadal variability in the atmosphere can superimpose on the mechanism described here but is unlikely to change it qualitatively.

Eden and Willebrand (2001) showed that changes in the wind stress field change the SPG circulation through a barotropic response on an intraseasonal time scale. On interannual time scales, a baroclinic response to the atmosphere ocean heat flux becomes more important. Because it is not subject to the fast atmospheric variability, we argue that oceanic heat and salt transports play an increasingly important role on decadal to multidecadal scales.

In this view the dynamics of the SPG depends on the overflow transport across the GSR. In the experiments presented the overflows are changed by a hydraulic overflow parameterisation. Nonetheless, complex OGCM's apply a range of other parameterisations that affect the overflow transport both in strength and density as for example bottom boundary layer models or mixing schemes (Thorpe et al., 2004). Further work is required to assess their influence on the SPG and to quantify the realistic influence of the overflows on the SPG circulation.

Acknowledgments

A.L. and J.M. were funded by the Gary Comer foundation. We are grateful to M. Hofmann for technical assistance on the overflow parameterisation.

Appendix A. Calculation of the depth integrated zonal transport equation

Consider the time independent momentum equation in meridional direction,

$$fu = -g\,\partial_y \eta + \partial_y \int_z^0 b'\,dz' + \rho_0^{-1}\,\partial_z \tau_{zy}, \tag{A-1}$$

with the average density ρ_0, gravitational acceleration g, Coriolis parameter f and the stress term τ_{zy} for a meridional force acting on the horizontal surface. b denotes the buoyancy

$$b = b(x,y,z) \equiv g\,\frac{\rho_0 - \rho}{\rho_0}; \quad b' = b(x,y,z'). \tag{A-2}$$

Splitting the buoyancy term in Eq. (A-1) into two parts simplifies the integration,

$$fu = -g\,\partial_y \eta + \partial_y \int_{-H}^0 b\,dz - \partial_y \int_{-H}^z b'\,dz' + \rho_0^{-1}\,\partial_z \tau_{zy}, \tag{A-3}$$

where H is the ocean depth. Integration yields the vertically integrated transport in zonal direction:

$$\begin{aligned} fM_x &\equiv f \int_{-H}^0 u\,dz \\ &= -g \int_{-H}^0 \partial_y \eta\,dz + \int_{-H}^0 dz\,\partial_y \int_{-H}^0 b\,dz - \int_{-H}^0 dz\,\partial_y \int_{-H}^z b'\,dz' \\ &\quad + \rho_0^{-1} \int_{-H}^0 dz\,\partial_z \tau_{zy} \\ &= -Hg\,\partial_y \eta + H\partial_y \int_{-H}^0 b\,dz + \partial_y \int_{-H}^0 z \cdot b\,dz + \frac{\tau_{0y}}{\rho_0}. \end{aligned} \tag{A-4}$$

Note that for the last step we used the Leibnitz Integral Rule,

$$\begin{aligned} &\int_{-H}^0 dz\,\partial_y \int_{-H}^z b'\,dz' \\ &= \partial_y \int_{-H}^0 dz \int_{-H}^z dz' b' - \int_{-H}^0 dz' b' \cdot \partial_y 0 + \int_{-H}^{-H} dz' b' \cdot \partial_y(-H) \\ &= \partial_y \int_{-H}^0 dz \int_{-H}^z dz' b', \end{aligned}$$

and integrated the result by parts. Thus, we identify:

$$P_b \equiv g\eta - \int_{-H}^0 dz'\,b',$$

$$\Phi \equiv -\int_{-H}^{0} dz \int_{-H}^{z} dz'\, b' = \left[-z \int_{-H}^{z} dz'\, b'\right]_{-H}^{0} + \int_{-H}^{0} dz\, z \cdot b$$
$$= +\int_{-H}^{0} dz\, z \cdot b.$$

The equation for the vertically integrated transport (A-4) can thus be written in terms of bottom pressure, $\rho_0 P_b$, and potential energy at depth H, $\rho_0 \Phi$:

$$fM_x = -H\partial_y P_b + \partial_y \Phi + \frac{\tau_{0y}}{\rho_0}. \tag{A-5}$$

References

Bacon, S., 1997. Circulation and fluxes in the North Atlantic between Greenland and Ireland. Journal of Physical Oceanography 27, 1420–1435.

Böning, C., Scheinert, M., Dengg, J., Biastoch, A., Funk, A., 2006. Decadal variability of subpolar gyre transport and its reverberation in the North Atlantic overturning. Geophysical Research Letters 33, L21S01.

Cane, M.A., Kamenkovich, V.M., Krupitsky, A., 1998. On the utility and disutility of JEBAR. Journal of Physical Oceanography 28, 519–526.

Clarke, R.A., 1984. Transport through the Cape Farewell-Flemish Cap section. Rapp. P.V. Reun. Cons. Int. Explor. Mer. 185, pp. 120–130.

Curry, R., McCartney, M., Joyce, T., 1998. Oceanic transport of subpolar climate signals to mid-depth subtropical waters. Nature 391, 575–577.

Dickson, R.R., Brown, J., 1994. The production of North Atlantic Deep Water: Sources, rates, and pathways. Journal of Geophysical Research 99 (12), 12319–12341.

Eden, C., Willebrand, J., 2001. Mechanism of interannual to decadal variability of the North Atlantic circulation. Journal of Climate 14, 2266–2280.

Fichefet, T., Maqueda, M.A.M., 1997. Sensitivity of a global sea ice model to the treatment of ice thermodynamics and dynamics. Journal of Geophysical Research 102, 12,60.

Gerdes, R., Köberle, C., 1995. On the influence of DSOW in a Numerical model of the North Atlantic general circulation. Journal of Physical Oceanography 25, 2624–2642.

Girton, J.B., Pratt, L.J., Sutherland, D.A., Price, J.F., 2006. Is the Faeroe Bank Channel overflow hydraulically controlled? Journal of Physical Oceanography 36, 2340–2349.

Gölzer, H., Mignot, J., Levermann, A., Rahmstorf, S., 2006. Tropical versus high latitude freshwater influence on the Atlantic circulation. Climate Dynamics 27, 715–725.

Greatbatch, R.J., Fanning, A.F., Goulding, A.D., Levitus, S., 1991. A diagnosis of interpentadal circulation changes in the North Atlantic. Journal of Geophysical Research 96 (22), 22009–22023.

Häkkinen, S., 2001. Variability in sea surface height: a qualitative measure for the meridional overturning in the North Atlantic. Journal of Geophysical Research 106 (13), 13837–13848.

Häkkinen, S., Rhines, P.B., 2004. Decline of subpolar North Atlantic circulation during the 1990s. Science 304, 555–559.

Hansen, B., Østerhus, S., 2000. North Atlantic–Nordic Seas exchanges. Progress in Oceanography 45, 109–208.

Hansen, B., Turrell, W.R., Østerhus, S., 2001. Decreasing overflow from the Nordic Seas into the Atlantic Ocean through the Faeroe Bank Channel since 1950. Nature 411, 927–930.

Hasumi, H., Suginohara, N., 1999. Effects of locally enhanced vertical diffusivity over rough bathymetry on the world ocean circulation. Journal of Geophysical Research 104 (23), 23364–23374.

Hátún, H., Sandø, A.B., Drange, H., Hansen, B., Valdimarsson, H., 2005. Influence of the Atlantic subpolar gyre on the thermohaline circulation. Science 309, 1841–1844.

Hofmann, M., Maqueda, M.A.M., 2006. Performance of a second-order moments advection scheme in an ocean general circulation model. Journal of Geophysical Research 111, C05006.

Kalnay, E. et al., 1996. The NCEP/NCAR 40-year reanalysis project. Bulletin of the American Meteorological Society 77, 437–471.

Käse, R.H., Oschlies, A., 2000. Flow through Denmark Strait. Journal of Geophysical Research 105 (28), 28527–28554.

Kösters, F., 2004. Denmark Strait overflow: comparing model results and hydraulic transport estimates. Journal of Geophysical Research 109, C10011.

Kösters, F., Käse, R.H., Schmittner, A., Herrmann, P., 2005. The effect of Denmark Strait overflow on the Atlantic Meridional Overturning Circulation. Geophysical Research Letters, 32.

Kuhlbrodt, T., Griesel, A., Montoya, M., Levermann, A., Hofmann, M., Rahmstorf, S., 2007. On the driving processes of the Atlantic Meridional Overturning Circulation. Reviews of Geophysics 45 (RG2001), 1–32.

Ledwell, J.R., Montgomery, E.T., Polzin, K.L., Laurent, L.C.S., Schmitt, R.W., Toole, J.M., 2000. Evidence for enhanced mixing over rough topography in the abyssal ocean. Nature 403, 179–182.

Levermann, A., Born, A., 2007. Bistability of the Atlantic subpolar gyre in a coarse resolution climate model. Geophysical Research Letters 34, L24605.

Levermann, A., Griesel, A., 2004. Solution of a model for the oceanic pycnocline depth: Scaling of overturning strength and meridional pressure difference. Geophysical Research Letters 31, L17302.

Levermann, A., Griesel, A., Hofmann, M., Montoya, M., Rahmstorf, S., 2005. Dynamic sea level changes following changes in the thermohaline circulation. Climate Dynamics 24, 347–354.

Levitus, S., 1982. Climatological Atlas of the World Ocean, NOAA Professional Paper, vol. 13. US Department of Commerce, Washington, DC.

Lohmann, G., 1998. The influence of a near-bottom transport parameterization on the sensitivity of the thermohaline circulation. Journal of Physical Oceanography 28, 2095–2103.

Mertz, G., Wright, D.G., 1992. Interpretations of the JEBAR term. Journal of Physical Oceanography 22, 301–305.

Mignot, J., Levermann, A., Griesel, A., 2006. A decomposition of the Atlantic meridional overturning circulation into physical components using its sensitivity to vertical diffusivity. Journal of Physical Oceanography 36, 636–650.

Mignot, J., Ganopolski, A., Levermann, A., 2007. Atlantic subsurface temperatures: response to a shut-down of the overturning circulation and consequences for its recovery. Journal of Climate 20, 4884–4898.

Montoya, M., Griesel, A., Levermann, A., Mignot, J., Hofmann, M., Ganopolski, A., Rahmstorf, S., 2005. The Earth System Model of Intermediate Complexity CLIMBER-3α. Part I: description and performance for present-day conditions. Climate Dynamics 25, 237–263.

Myers, P.G., Fanning, A.F., Weaver, A.J., 1996. Jebar, bottom pressure torque, and gulf stream separation. Journal of Physical Oceanography 26, 671–683.

Penduff, T., Barnier, B., de Verdière, A.C., 2000. Self-adapting open boundaries for a sigma coordinate model of the eastern North Atlantic. Journal of Geophysical Research 105 (11), 11279–11298.

Petoukhov, V., Ganopolski, A., Brovkin, V., Claussen, M., Eliseev, A., Kubatzki, C., Rahmstorf, S., 2000. CLIMBER-2: a climate system model of intermediate complexity. Part I: model description and performance for present climate. Climate Dynamics 16, 1.

Prather, M.J., 1986. Numerical advection by conservation of second-order moments. Journal of Geophysical Research 91, 6671–6681.

Rahmstorf, S., 1996. On the freshwater forcing and transport of the Atlantic Thermohaline Circulation. Climate Dynamics 12, 799–811.

Redler, R., Böning, C.W., 1997. Effect of the overflows on the circulation in the subpolar North Atlantic: a regional model study. Journal of Geophysical Research 102 (18), 18529–18552.

Riemenschneider, U., Legg, S., 2007. Regional simulations of the Faeroe Bank Channel overflow in a level model. Ocean Modelling 17, 93–122.

Roberts, M.J., Wood, R.A., 1997. Topographic Sensitivity Studies with a Bryan Cox-Type Ocean Model. Journal of Physical Oceanography 27, 823–836.

Sarkisyan, A.S., Ivanov, V.F., 1971. Joint effect of baroclinicity and bottom relief as an important factor in the dynamics of sea currents. Izvestiya Akademii Nauk SSSR Fizika Atmosfery i Okeana 7 (2), 173–188.

Spall, M.A., 2004. Boundary currents and Watermass transformation in marginal seas. Journal of Physical Oceanography 34, 1197–1213.

Straneo, F., 2006. On the connection between dense water formation, overturning, and poleward heat transport in a convective basin. Journal of Physical Oceanography 36, 1822–1840.

Thorpe, R.B., Wood, R.A., Mitchell, J.F.B., 2004. Sensitivity of the modelled thermohaline circulation to the parameterisation of mixing across the Greenland–Scotland ridge. Ocean Modelling 7, 259–268.

Treguier, A.M., Theetten, S., Chassignet, E.P., Penduff, T., Smith, R., Talley, L., Beismann, J.O., Böning, C., 2005. The North Atlantic subpolar gyre in four high-resolution models. Journal of Physical Oceanography 35, 757–774.

Vellinga, M., Wood, R.A., 2002. Global climatic impacts of a collapse of the Atlantic thermohaline circulation. Climatic Change 54, 251–267.

Whitehead, J.A., Leetma, A., Knox, R.A., 1974. Rotating hydraulics of strait and sill flows. Geophysical Fluid Dynamics 6, 101–125.

Wood, R.A., Keen, A.B., Mitchell, J.F.B., Gregory, J.M., 1974. Changing spatial structure of the thermohaline circulation in response to atmospheric CO_2 forcing in a climate model. Nature 399, 572–575.